PREPRINT
Submitted to the 6th International Symposium on Fusion Nuclear Technology
San Diego, April 2002

Modeling infinite/axisymmetric liquid metal magnetohydrodynamic free surface flows

Neil B. Morley[1], Sergey Smolentsev, and Donghong Gao
Mechanical and Aerospace Engineering Department, University of California Los Angeles, USA

Abstract

Over the past several years, as part of the APEX and ALPS projects, liquid metal magnetohydrodynamic film and jet flows have been modeled using the assumption of axisymmetry to simplify the governing equations to a more tractable two-dimensional form. The results of these two-dimensional simulations as it pertains to the liquid wall and divertor flows is presented here. The effect of toroidal field gradient on the flow thickness is shown to be rather small for thin fast first wall flows on electrically insulated backwalls, but streamwise currents generated by flow across the toroidal field gradient can interact with radial magnetic field components to produce toroidal motion with strong shear across the flow depth. The drag effects from flow across the toroidal field gradients become much stronger if thicker flows are considered. Concerns about surface stability due to forces trying to pull the liquid off the backwall also become much more severe for thicker flows or flows with conducting walls. Plans for continued work with three-dimensional models are discussed.

1. Introduction

Liquid Metal (LM) flows with a free surface in a magnetic field are used in several different engineering applications. As examples we can refer to metallurgical processes, such as continuous casting of steel, where the liquid motion is controlled by a static magnetic field [1], and especially to liquid wall flows in a fusion reactor. Recently, the liquid wall concept has had a significant place in the Advanced Power Extraction (APEX) study [2]. For example, in the CLiFF (Convective Liquid Flow First-Wall) design, which is a part of the APEX study, liquid metal, such as Lithium (Li) or Tin (Sn), is injected poloidally at some location in the plasma chamber to form a thin flowing film. The layer moves over the reactor walls, and then the liquid is removed in some fashion from the chamber. The attractiveness of this idea stems from the removal of high surface heat loads, protection of the reactor First Wall (FW) from sputtering erosion, and elimination of peak thermal stresses in solid FW components [2].

However, practical realization of this idea requires detailed knowledge of the free surface flow behavior over complex geometry guiding structures and in the presence of strong magnetic fields. The magnetic field in a real reactor environment exhibits both temporal and spatial variations and generally has three components with respect to the main flow direction. In addition, the toroidal shape of a classic tokamak reactor has double curvature, in the poloidal and toroidal directions. In spite of the diversity of tokamak configurations, however, the common feature of all basic designs is the near-toroidal symmetry of the reactor vacuum chamber and reactor field that allows liquid wall concepts with no toroidal breaks to be treated as axisymmetric, with no variation with the toroidal coordinate. While the assumption of axisymmetry is an idealization – real reactors require penetrations for plasma fueling and heating, and inlets and outlets for liquid flow that thread between toroidal field coils – it is a powerful tool for simplifying the magnetohydrodynamic (MHD) equations to a two-dimensional form.

Over the past couple years, the assumption of axisymmetry has been used for the modeling of flows related to the APEX design concepts, where special attention has been paid to MHD effects in liquid walls caused by the streamwise variations of the toroidal magnetic field, multiple field components, and curved wall topology, without referring to a particular design. This work, which has been reported at APEX meetings, but has been largely unpublished, is reported here.

To our knowledge, the theoretical data published on free surface flows in non-uniform magnetic fields are scarce and restricted to jet flows [3] or film flows in particular fusion applications [4]. It should be noted that various studies have been performed for non-uniform MHD flows in closed channels caused by a space-varying magnetic field, changes of the flow orientation or variation of the cross-sectional area. Detailed review of these studies has been presented in

[1] Corresponding author, morley@fusion.ucla.edu

classic books on MHD [5,6,7] and journal papers [8]. Both magnetic field and geometry variations give rise to a streamwise electric potential differences, which drives current in the downstream direction. These currents, while interacting with the magnetic field, produce electromagnetic forces driving the liquid from the core to the channel periphery resulting in the "M-shaped" velocity profile and increased MHD pressure drop. Similar effects and new ones manifesting themselves in the changes of the flow thickness can be expected in flows with a free surface but their theoretical analysis is more complicated because of the need of calculating the free surface location simultaneously with the other flow variables.

2. Axisymmetric governing equations

In general we will use the terms "axisymmetric" and "infinite" in an interchangeable way. In reality axisymmetric flows will have some element of curvature associated with them, but for the most part we will assume that curvature is small and approximate such flows in Cartesian geometry with the x-y plane representing the poloidal plane, and with z in the toroidal direction. (A more general model formulation that accounts for curvature effects is described in [12])

For axisymmetric flows then we make the assumption that $\partial/\partial z = 0$ to simplify the Navier-Stokes equations. The convenience of the axisymmetic assumption in MHD is that it decouples the effect of magnetic fields applied in the direction of the axisymmetry (toroidal) form those in the poloidal plane. The governing equations in 2D axisymmetric form can be written as:

$$\frac{D\vec{v}}{Dt} = -\frac{1}{\rho}\nabla_\perp p + \nu\nabla_\perp^2\vec{v} + \vec{g} + \\ + \frac{1}{\rho}\left(\vec{j}_\perp \times B_z\hat{z} + j_z\hat{z}\times\vec{B}_\perp\right) + \frac{1}{\rho}\vec{j}_\perp\times\vec{B}_\perp \quad (1)$$

$$\nabla_\perp\cdot\vec{v} = 0 \quad (2)$$

where *v*, *p*, and *B* are the velocity, pressure and applied magnetic induction; $\perp$ denotes the x-y plane; D/Dt is the convective derivative; and ρ, υ are the density, kinematic viscosity and acceleration of gravity all assumed constant in this work. This formulation keeps all three components of the velocity and magnetic field. The magnetic terms are separated in such a way to show forces acting in the poloidal plane (1st term) and forces acting in the toroidal direction (2nd term).

The model of electric currents can be approached most effectively following a hybrid approach, where $j_\perp$ is calculated from a stream function, and j_z is calculated from Ohm's Law:

$$\vec{j}_\perp = \nabla\times H\hat{z} \quad j_z = \sigma\left(\vec{v}_\perp\times\vec{B}_\perp\right) \quad (3a,b)$$

where *H* is the stream function for poloidal current (*i.e.* the z-directed induced magnetic field intensity due to poloidal currents) and σ is the electrical conductivity of the LM. Eq. (3b) is sufficient for the calculation of j_z since in an axisymmetric 2D flow the electric field drops out, as toroidal currents are able to loop around the entire torus. But an induction type equation is necessary for *H* and can be formulated based on the z-component of the curl of Ohm's Law, giving:

$$\frac{1}{\sigma}\nabla^2 H = \left(\vec{v}\cdot\nabla_\perp\right)B_z - \left(\vec{B}\cdot\nabla_\perp\right)w \quad (4)$$

It is assumed here for the presentation of the equations that the induced magnetic field is small compared to the applied field, but this is not necessarily true in all cases (some of the numerical formulations utilized later in fact do not make this assumption).

The equations can be made dimensionless by a judicious selection of characteristic values, U*, B*, L*, L*/U*, $\rho(U^*)^2$, $\sigma^*U^*B^*$, $\sigma L^*U^*B^*$ for velocity, applied field, length, time, pressure, current density, and induced magnetic field intensity giving the following system:

$$\frac{Du}{Dt} = -\frac{\partial p}{\partial x} + \frac{\nabla_\perp^2 u}{\mathrm{Re}} + \frac{\sin\theta}{\mathrm{Fr}} + \frac{\mathrm{Ha}^2}{\mathrm{Re}}(j_y B_z - j_z B_y)$$
$$\frac{Dv}{Dt} = -\frac{\partial p}{\partial y} + \frac{\nabla_\perp^2 v}{\mathrm{Re}} - \frac{\cos\theta}{\mathrm{Fr}} + \frac{\mathrm{Ha}^2}{\mathrm{Re}}(j_z B_x - j_x B_z)$$
$$\frac{Dw}{Dt} = \frac{\nabla_\perp^2 w}{\mathrm{Re}} + \frac{\mathrm{Ha}^2}{\mathrm{Re}}(j_x B_y - j_y B_x) \quad (5a\text{-}h)$$
$$\frac{\partial u}{\partial x} + \frac{\partial v}{\partial y} = 0$$
$$\nabla_\perp^2 H = u\frac{\partial B_z}{\partial x} + v\frac{\partial B_z}{\partial y} - B_x\frac{\partial w}{\partial x} - B_y\frac{\partial w}{\partial y}$$
$$j_x = \frac{\partial H}{\partial y}, \quad j_y = -\frac{\partial H}{\partial x}, \quad j_z = \sigma\left(uB_y - vB_x\right)$$

where θ(x,y) is the local angle of the flow to gravity. Deviations from this standard model (due to toroidal curvature for instance) will be noted as needed.

3. Effect of spatially varying toroidal magnetic field

Focus is placed in this section solely on the effect of variations in the toroidal field, with contributions of other field components neglected, so that $\vec{B} = (0, 0, B_z(x, y))$ is assumed. In this case, there is no source for motion or current in the toroidal direction (w, $j_z = 0$) and Eq. (5e) for the induced magnetic field takes on the form:

$$\nabla_\perp^2 H = u\frac{\partial B_z}{\partial x} + v\frac{\partial B_z}{\partial y} \qquad (6)$$

What is notable from the form of Eq. (6) is that the behavior of the induced field is governed by standard diffusion with a source term that depends on the spatial (and temporal in a more complete treatment) variations in the applied field. In Cartesian geometry, if there is no variation in the applied field, then there is no MHD effect on the flow in this two-dimensional treatment. What we have effectively done, is removed the effects of Hartmann layers so that only the effects of the gradients are studied.

3.1 Fully developed film flow

It is possible to gain insight into some of the behavior of this field gradient by exploring a special case where $B_z(x,y) = C \cdot x$. In this case of an infinite linear gradient of the applied field with constant strength C, the governing equations reduced to:

$$\nabla_\perp^2 u = -\mathrm{Ha}^2 H - \frac{\mathrm{Re}}{\mathrm{Fr}}\sin\theta$$
$$\nabla_\perp^2 H = u \qquad (7a,b)$$

where the characteristic field used in the definition of Ha is based on the gradient B* = C·L*, and not on any local value of the field.

The solution of Eqs. (7) is lengthy and is covered in detail in [9], but as can be inferred from the equations, the resultant mass flow depends only on the gradient value. It is this fact that allows a fully developed solution to be reached at all. Also notable is that the induced current is only streamwise, meaning there are no direct $\boldsymbol{J}\times\boldsymbol{B}$ retarding forces, only forces acting perpendicular to the main flow direction. These forces create a pressure profile that in turn affects the streamwise flow in drastic ways, depending on the strength of the applied field gradient. The velocity profiles for several values of Ha are shown in Fig. 1, were at high Ha we see the formation of the free surface equivalent of the M-shaped velocity profile with boundary jet thickness scaling with √Ha (where Ha is based on the gradient!).

This lop-sided M-shaped velocity is driven purely by the pressure gradient effects, and is the result of the same physical effect as the so-called magnetic propulsion idea [10] proposed to aid in-situ pumping of free surface flows. In the magnetic propulsion scheme, a streamwise flow of applied electrical current is injected into the film flow. This current is oriented such that it pushes the liquid against the supporting wall (which could in theory be inverted to gravity), and due to gradient in the field strength (or the current density itself) provides a pressure gradient that propels the flow along. This current is easily added to this analysis as a change in boundary condition on the induced field, and gives changes in the velocity profile as shown in Fig. 2. Because the strongest portion of the pressure gradient is near the back wall, the flow is accelerated predominantly in this region, with relatively slower flow near the surface. While this type of velocity profile is not ideal for heat transfer, it remains to be seen how quickly such a profile will developed, and how stable such a flow will remain. It is well known that such side layers in closed channel flow (for which this theory is equally applicable) are unstable and lead to enhanced mixing near the rigid boundaries [11].

3.2 Developing film and jet flows

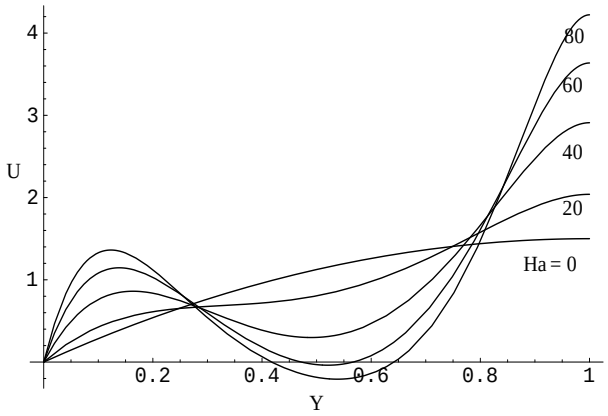

Figure 1. Fully developed velocity profiles for flow in a linear gradient field of various strength

Several numerical models [12,13,14] with different formulations have been developed to solve the developing flow Eqs. (5) using the height function free surface tracking method for film flows and using a volume of fluid free surface tracking method for films and 2D jets. The codes have been applied to several typical fusion geometries, specifically flow along a first wall, flow along divertors, and flow in partially full exit pipes, to assess the impact of strong field gradients on such liquid components (see Table 1). Only a portion of the results can be included here, but some general conclusion can be reached based on the modeling data.

Typical outboard liquid first wall cases, in a reactor the scale of ARIES-RS [15], will experience an average gradient in the range of 0.25 to 1 T/m depending on the

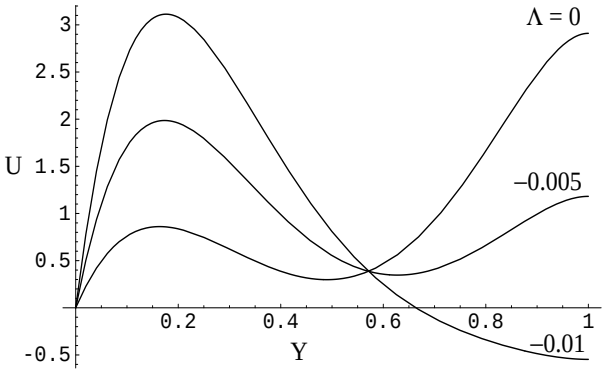

Figure 2. Fully developed velocity profiles for flow in a linear gradient field at Ha = 40 with various applied streamwise current strengths $\Delta = I_a \mu_m / B^*$

Table 1. Summary of flow cases analyzed for Li / Sn

	h (cm)	U (m/s)	∇B_z (T/m)	Ha ($\nabla B h^2 \sqrt{\sigma/\rho\nu}$)	Re (Uh/ν)
First Wall	2	10	.25	9/ 3.25	2.4×10^5/ 1×10^6
Exit Pipe	20	1	10	3.6×10^4/ 1.3×10^4	2.4×10^5/ 1×10^6

first wall geometry assumed. For the circular arc outboard flow geometry of Fig. 3 and field profile shown in Fig. 4, the lithium flow depth (Fig. 5) is affected only slightly by the field gradient drag effect[1]. The drag effect can be slightly stronger for conducting walls and much stronger for thicker or slower flows. When an alternate liquid like Sn is considered, the drag effect is much reduced due to the greater density (inertia) of Sn, and for these conditions no change in field height is observed.

While this result is positive, there is a concern that arises from the fact that the streamwise currents flow in one direction near the surface and in the opposite direction near the back wall (see Fig 5). This current pattern results in a force near the surface that tries to pull the liquid into the plasma. This force integrates to zero over the entire depth of the liquid film if the back wall is insulated, but may have implications on the surface stability of the flow [9]. If the back wall is conducting, there will be a net force pulling or pushing the liquid relative to the wall [16] and issues of flow detachment arise.

Modeling of this stability effect is continuing, but some initial results for first wall flows at relatively low Reynolds Number are shown in Fig. 6, where a small perturbation in a Sn flow grows rapidly in the 1/R field gradient. For Li the disturbances develop even faster. Increasing the velocity slows down this process considerably, and Sn has been shown to be relatively stable for the first wall parameters listed in Table 1.

Another fusion relevant case, that of gravity flow out of drain pipe between toroidal magnetic field coils, experiences a considerably more dramatic effect owing to the large field gradient, see Table 1. While the assumption of an infinite channel is not as applicable to flows of this type, it is still useful to observe the strong effect on such flows, and realize that the actual drag

[1] Note that this calculation includes the effect of expanding/contracting flow area that requires a rather complicated generalization of Eqs. (5).

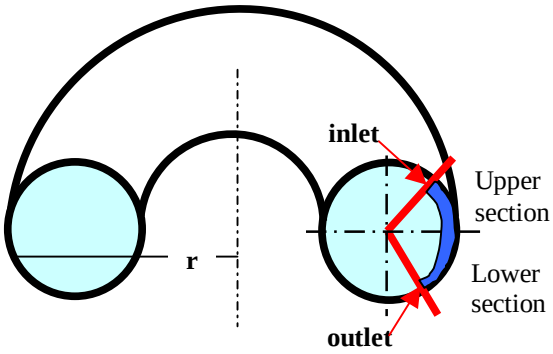

Figure 3. Outboard first wall flow geometry

will be stronger due to the neglected Hartmann drag effect. This work is covered in detail in [17], but a typical case given in Fig. 7 depicts the violent stability and drag effect that comes from flow through such a strong field gradient.

The so-called magnetic propulsion current discussed earlier can be added to both of the above cases. Calculations (see Fig. 8) and recent experiments have shown this current to be very effective in pushing the liquid against the back wall, aiding in liquid propulsion, and suppressing surface instabilities – potentially overcoming several of the problems discussed above for both first wall and drain pipes. The most serious problem encountered with the magnetic propulsion idea is the effect of other field components (see next section) on the flow dynamics.

Electrical conductivity of the back wall in general does not make the drag significantly worse for these

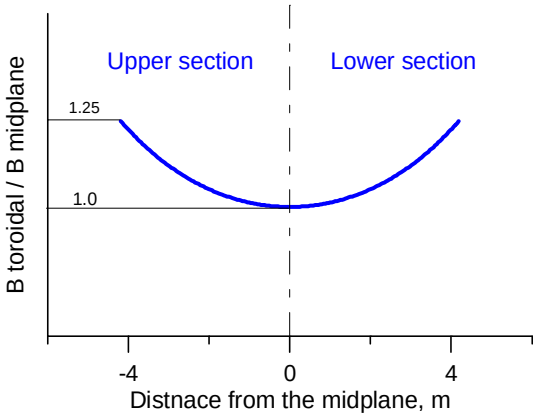

Figure 4. Typical normalized variation of magnetic field over outboard first wall (see Fig. 3)

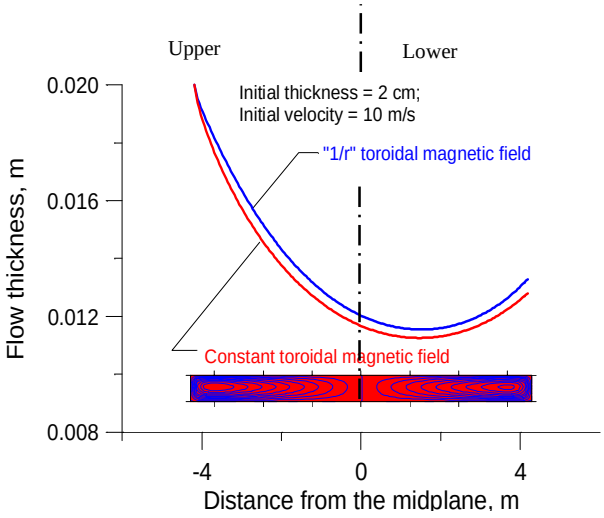

Figure 5. Effect of toriodal field gradient on depth of first wall flow (see Table 1) and poloidal current contours

axisymmetric flows, but it can exacerbate the stability and detachment issues since the net force on the liquid can act to pull the film off of the back wall. Another concern is the effect of electrically conducting nozzles and collectors, as pointed out in [18]. Locally providing a path for current closure in the near nozzle region might significantly affect the shape of jets and

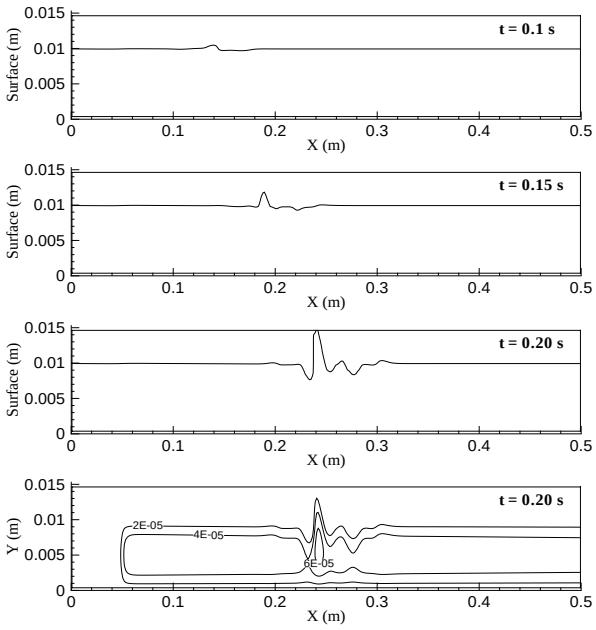

Figure 6. Growth of small disturbance on Sn first wall flow with Ha=7 and Re=5x10^4

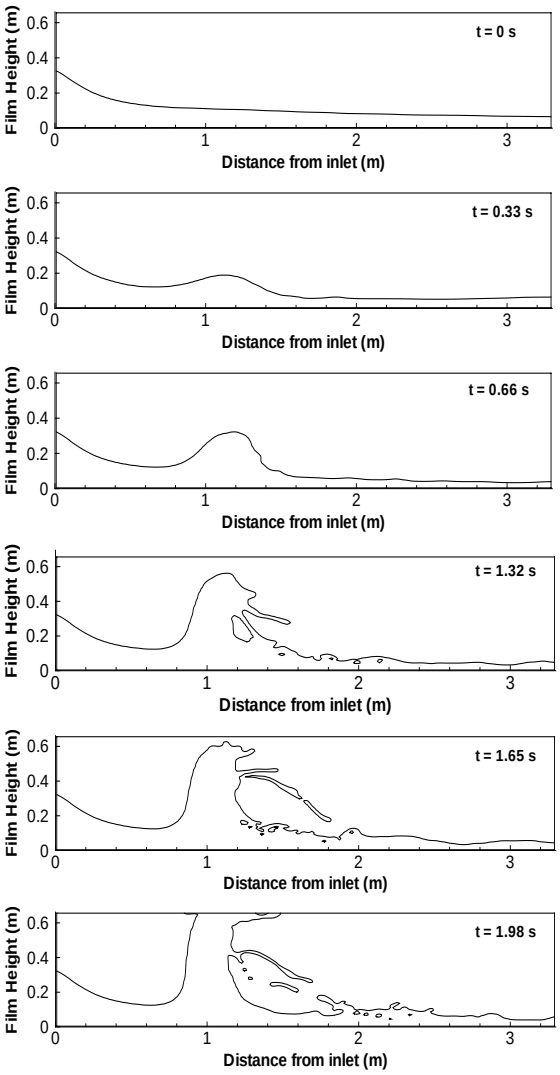

Figure 7. Free surface flow in exit pipe through a very strong field gradient (from [17])

films as they emerge from the nozzle and become free surface flows. This problem can be modeled with the 2D tools described above, and future will investigate this effect in more detail.

4. Three component magnetic field

The MHD effects become even more interesting as one adds additional field components and observes the

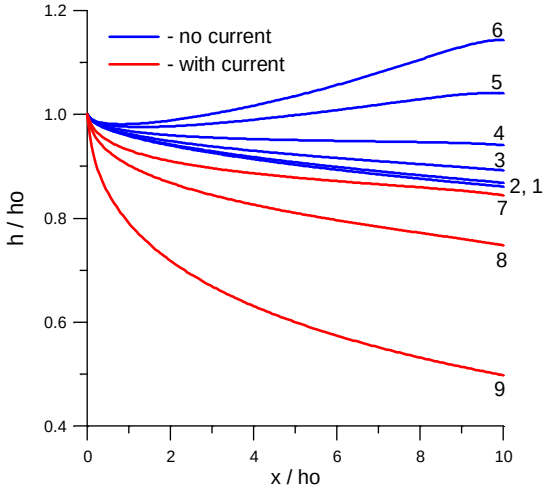

Figure 8. Height of free surface flows in increasingly strong field gradient (lines 1-6), and then with increasing magnetic propulsion current (lines 7-8) for strongest gradient case.

interaction of various components of field and induced current. If a radial field component is added to a constant toroidal magnetic field, then in the axisymmetric case, the two components do not interact. Motion in poloidal plane does not produce any current due to the constant toroidal field (except maybe near conducting nozzles [18]), and the current created by the poloidal motion in the radial field produces only toroidal current. This toroidal current however will interact with the radial field to produce a strong drag effect. Since the assumption of axisymmetry provides a complete toroidal flow path for this toroidal current, no electric field can arise to oppose the current (see Eq. 3b) – meaning that the flow behaves like flow in a perfectly conducting channel. Some calculations done for APEX to determine the strength of radial field that can be tolerated before doubling the flow depth (halving the original velocity) are shown in Fig. 9. For Li flows similar to those discussed before, the tolerable surface normal field is ~0.018T (for Sn it is closer to 0.08T). Recent work [19] for jet flows has shown that this tolerable (doubling) surface normal field (neglecting gravitational and viscous effects) scales like:

$$\text{Max } B_n = \sqrt{\frac{\rho U}{2\sigma L}} \qquad (8)$$

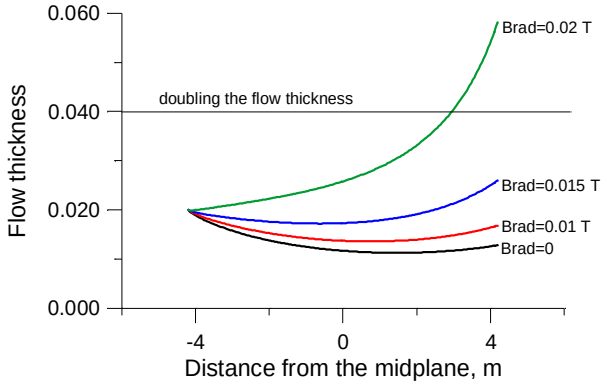

Figure 9. Thickening of Li first wall flow due to various strengths of radial magnetic field

where L is the flow distance under consideration. This formula compares fairly well against the numerical predictions for film flows cited above as well. The conductivity of the back wall does not affect these results, unless one considers inserting toroidal breaks of the axisymmetry.

Considering now the case with both radial and toroidal field components when the toroidal field has a gradient, a new phenomena – toroidal motion – is seen. The streamwise current induced by the gradient in the toroidal field can interact with perpendicular radial field to produce toroidal forces (see Eq. 5c) accelerating the flow toroidally around the torus. Since, as noted before, the streamwise current changes direction as one travels along the film depth, the direction of the toroidal force also changes so that near the backwall the liquid is moving in one direction, and near the surface in the opposite direction, with strong shear in between. Fig. 10 shows the resultant toroidal velocity profiles for a Sn flow in the same geometry and field distribution as Figs. 3-4, assuming a steady radial field component of 0.05 T. As one can see in the figure, quite large toroidal velocities can develop, on the order of a few tenths of a meter per second. For lithium flows (not pictured) the velocities are roughly 5 times higher.

The use of streamwise magnetic propulsion currents in a case with radial field components will preferentially push the liquid in the toroidal/anti-toroidal direction depending on the sign of the radial field. For an axisymmetric flow, these types of toroidal motions are acceptable. But if one considers toroidal breaks of any kind, liquid splashing and non-uniformity can result.

As a final case, if one considers both a radial and streamwise components of the applied field, the toroidal current induced by the motion across the radial field will interact with the the streamwise field to either push the liquid against the back wall, or pull it up. We have not done many simulations of this particular case, but the force of detachment can be quite large in these instances and needs to be more fully quantified.

5. Conclusions

While this significant amount of work on axisymmetric models has been informative, and revealed both unexpected qualitative trends and hard quantitative flow height predictions, one must not forget that deviations from axisymmetry will be important. Even one toroidal break around the reactor torus is likely to have strong effects on the flow dynamics due to the reintroduction of that Hartmann effect due to the strong toroidal field and blockage of toroidal motion of the liquid films. To truly accommodate penetrations, inlet nozzles and outlet diffusers, deflectors and drain channels, a 3D modeling capability that can accommodate spatially varying fields and complex geometry structures must be developed for use in the APEX and ALPS projects. Such tools are currently under development and already

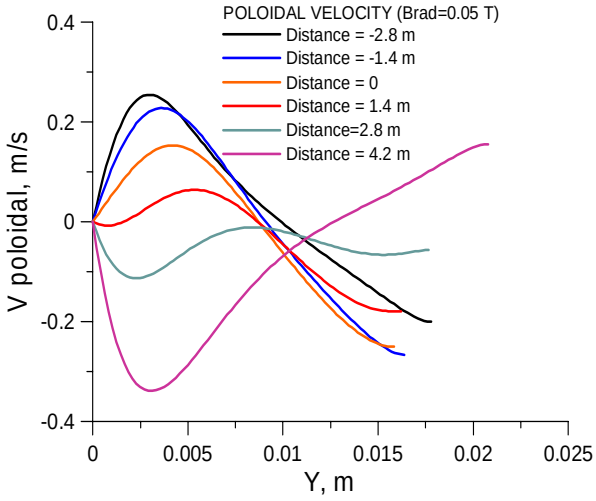

Figure 10. Toroidal velocity profiles over liquid depth for liquid Sn flow in toroidal field gradient and constant radial field

yielding limited 3D results. In particular we note the efforts by the HYPERCOMP [14] group to develop and unstructured grid 3D free surface MHD solver that, if successful, will have a serious impact on our understanding and predictive capability of liquid wall and divertor flows for fusion.

In addition, new experiments are also necessary to provide data for liquid wall designers and modelers. The MTOR facility, for example [20], is a magnetic torus, liquid metal flow loop facility capable of exploring large volume liquid metal free surface flows in toroidal field gradients and multiple component magnetic fields. Such data is crucial to the validation of the modeling effort reported here.

Acknowledgements

The authors would like to acknowledge the support of the APEX project through DOE Grant DE-FG03-86ER52123.

References

1. A.F.Lehman, G.R.Tallbäck, and H.R.Hackl, "Fluid flow control in continuous casting using various configurations of static magnetic fields," in *Proceedings of International Symposium on Electromagnetic Processing of Materials*, 25-28 Oct. 1994 (ISIJ, Nagoya, Japan, 1994), 372-377.
2. M.Abdou, The APEX Team, "On the exploration of innovative concepts for fusion chamber technology," Fusion Engineering and Design, **54**, 181-247 (2001).
3. S.Oshima, R.Yamane, Y.Mochimaru, T.Matsuoka, "The shape of a liquid metal jet under a non-uniform magnetic field," JSME Int.J., **30**, 437-448 (1987).
4. A.Ying et al. "MHD and heat transfer issues and characteristics for Li free surface flows under NSTX conditions," Fusion Technology, **39**, 739-745 (2001).
5. J.A.Shercliff, "*A textbook of magnetohydro-dynamics*," Pergamon Press, Oxford, p.265 (1965).
6. H.Branover, "*Magnetohydrodynamic flows in ducts*," John Willey & Sons, New York, p.290 (1978).
7. R.Moreau, "*Magnetohydrodynamics*," Kluwer Academic Publisher, p.313 (1990).
8. I.R.Kirillov, C.B.Reed, L.Barleon, K.Miyazaki, "Present understanding of MHD and heat transfer phenomena for liquid metal blankets," Fusion Engineering and Design, **27**, 553-569 (1995).
9. D.Gao and N.B. Morley, *Equilibrium and initial stability analysis of liquid metal falling film flows in a varying spanwise magnetic field*, Submitted to Magnetohydrodynamics, 2002.
10. L.Zakharov et al. "Magnetic propulsion of conducting fluid and the theory of controlled tokomak fusion reactor," *Meeting on Liquid Lithium, Controlled Tokamak Fusion Reactors & MHD, Int. Sherwood Fusion/Plasma Conference*, Atlanta GA, March 21, 1999.
11. N.B.Morley, S.Smolenstev, L Barleon, I.Kirillov, M.Takahashi, *"Liquid Magnetohydro-dynamics: Recent work and future directions for fusion"*, Fusion Engineering and Design, Vol. 51-52, pp. 701-713, 2000
12. S.Smolentsev M.Abdou, T.Kunugi, N.Morley, S.Satake, A.Ying, *"Modeling of liquid walls in the APEX study,"* To appear in International Journal of Applied Electromagnetics and Mechanics, 2002.
13. APEX Interim Report, UCLA-FNT-107, 1999.
14. APEX Presentations by S. Smolentsev, N. Morley, H.Huang, A.Ying, D. Gao, R. Munipalli, available at http://www.fusion.ucla.edu/APEX, 1998-2002.
15. M.S.Tillack et al. Configuration and engineering design of the ARIES-RS tokamak power plant. Fusion Engineering and Design, vol.38, (no.1-2),. p.87-113. 1997.
16. A.Y.Aydemir, *"Effects of liquid metal walls on equilibrium and stability in tokamaks"*, University of Texas Institute of Fusion Studies, Report IFSR-916, 2000.
17. D.Gao, N.B.Morley, M.Abdou, *"Numerical study of liquid metal film flow in a varying spanwise magnetic field,"* These Proceedings, 2002.
18. I.Konkashbaev, A.Hassanien, "MHD Problems in free liquid surfaces as plasma-facing materials in magnetically confined reactors," These Proceedings, 2002
19. S.Molokov, C.Reed, "*Flow of a two-dimensional liquid metal jet in a strong magnetic field*," These Proceedings, 2002
20. N. B. Morley, *"Experimental investigations of free surface stability and heat transfer for liquid for liquid metal and molten salt systems,"* IWIC-PIC, Japan, May 2002.